Vol 13 No 9, September 2004
1009-1963/2004/13(09)/1510-06

Chinese Physics

© 2004 Chin. Phys. Soc.
and IOP Publishing Ltd

Study of particle behaviour at the edge in HT-7 tokamak*

Xu Wei(徐 伟)[a)b)], Wan Bao-Nian(万宝年)[a)], Zhou Qian(周 倩)[a)]
Wu Zhen-Wei(吴振伟)[a)†], Mao Jiao-Shan(毛剑珊)[a)], and Li Jian-Gang(李建刚)[a)]

[a)] *Institute of Plasma Physics, Chinese Academy of Sciences, Hefei* 230031, *China*

[b)] *Department of Physics, Guangzhou University, Guangzhou* 510405, *China*

(Received 24 August 2003; revised manuscript received 26 April 2004)

The cross-field diffusion coefficient ($D_\perp$) at the edge in the HT-7 tokamak is close to the Bohm value when the line average electron density ranges from 1.5×10^{19} to $3.0\times10^{19}\mathrm{m}^{-3}$. The energy profile of the particles is derived directly from the $H_\alpha(D_\alpha)$ line shape; the dissociative excitation of molecules is dominating when the local electron temperature is above 10eV. By means of the Monte Carlo method the D_α line shape is also simulated. We find that the molecular dissociation contributes to 57% of neutral atoms and 53% of emission intensity in front of the limiter, and 85% of neutral atoms and 82% of emission intensity in front of the wall. The influence of atomic and molecular processes on the energy balance is discussed for the scrape-off layer (SOL), and the power loss from molecular dissociation is found to be 6×10^4kW at the SOL. The ion Bernstein wave (IBW) can effectively suppress the magnetohydrodynamic behaviour, the fluctuation levels and the turbulence; the $D_\perp$ in front of the limiter declines from 0.84 to $0.2\mathrm{m}^2\cdot\mathrm{s}^{-1}$ and the particle confinement time rises from 9 to 12ms.

Keywords: plasma, diffusion coefficients, energy profile, atomic and molecular processes, simulation of D_α line shape

PACC: 5255, 5225p, 5235

1. Introduction

It is already evident that tokamak operation are largely controlled, or even dominated, by edge processes. The particle confinement, electron density and impurity density depend strongly on the condition at the edge. The edge condition plays a key role in producing the H-mode, improving ohmic and super shot modes. But diagnosis of the edge has been much less extensive than that of the central part, and the experimental database of the edge is also very limited. In this paper, a number of important plasma parameters at the edge obtained by an optical method and a Langmuir probe array are presented. The result can describe the basic image of the edge in HT-7 tokamak.

2. Experiment

HT-7 is a superconducting tokamak,[1] with major radius R=1.22m and minor radius a=27.5cm, defined by a full circular limiter in the circular cross section. Twenty-four superconducting coils can create and maintain a toroidal magnetic field up to 2.5T. The recent operational parameters are plasma current 100–250kA, toroidal field 1.0–2.5T, line-averaged electron density ($\bar{n}_\mathrm{e}$) 8×10^{18}–$6\times10^{19}\mathrm{cm}^{-3}$, and electron temperature (T_e) 0.5–1.5keV. The main diagnostic systems on HT-7 tokamak have been described in Ref.[2].

Two sets of vertical multi-channel diode arrays are used to measure the distribution of $H_\alpha(D_\alpha)$ radiation in front of the limiter and the wall separately. The $H_\alpha(D_\alpha)$ line shape is measured by two sets of optical spectroscopy multi-channel analysers (OMAs).[3] The spectral dispersions of the system, equipped with a 1200 lines mm^{-1} grating and a 3600 lines mm^{-1} grating, are 0.023nm pixel^{-1} and 0.057nm pixel^{-1} respectively. The experimental arrangement is shown Fig.1.

*Project supported by the National Natural Science Foundation of China (Grant Nos 19775013 and 10275014).
†E-mail:gnuxuwei@163.net.

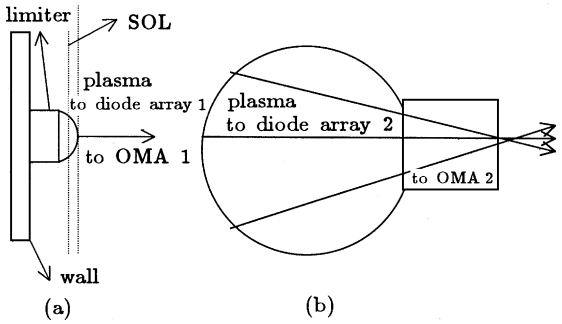


Fig.1. Experimental setup for the measurement of the emission and the distribution of $H_\alpha(D_\alpha)$ in front of the limiter (a) and the wall (b).

3. The plasma parameters at the edge

The profiles of electron temperature and density at the edge can be measured with a Langmuir probe, which has a spatial resolution of 1mm. The result is shown in Fig.2. The scrape-off lengths of T_e and n_e, λ_e and λ_n can be derived directly from the profiles of T_e and n_e at the edge.[4] For a simple scrape-off layer (SOL), where the cross-field transport is the only source term and the limiter is the only sink term, the cross-field diffusion coefficients can be written as $D_\perp = \lambda_n^2 c_s/(2L_c)$,[5] where $L_c \approx 0.75q\pi R$ is the connection length, $c_s = (kT_e/m_i)^{1/2}$ is the ion acoustic velocity, and the radial variation of c_s has been neglected. On the other hand, according to so-called Bohm diffusion formula, an empirical diffusion coefficient is $D_\perp^{\rm Bohm} = 0.06T/B$, where T is the plasma temperature and B is the magnetic field. The evolution of $D_\perp$ and $D_\perp^{\rm Bohm}$ with $\bar{n}_e$ is shown in Fig.3. It is obvious that $D_\perp$ in the SOL is close to the Bohm value of 0.45–0.82$\rm m^2\cdot s^{-1}$ when $\bar{n}_e$ ranges from 1.5×10^{19} to $3.0\times10^{19}\rm m^{-3}$ in HT-7. $D_\perp^{\rm Bohm}$ reduces almost linearly with increasing density, because the electron temperature at the edge decreases linearly with increasing $\bar{n}_e$.

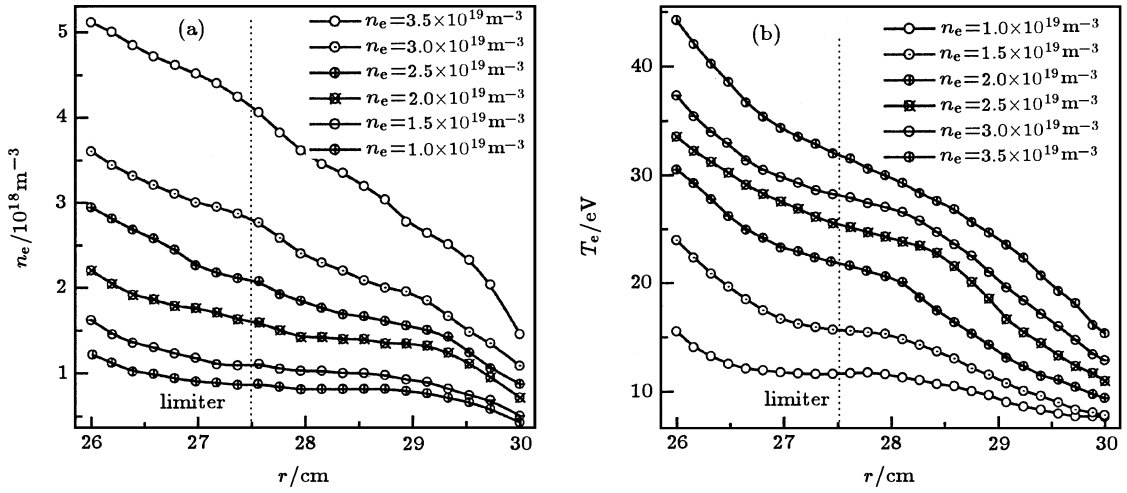


Fig.2. The profile of the electron density (a) and temperature (b) at the edge, with $\bar{n}_e/10^{19}\rm m^{-3}$=1, 1.5, 2, 2.5, 3, 3.5.

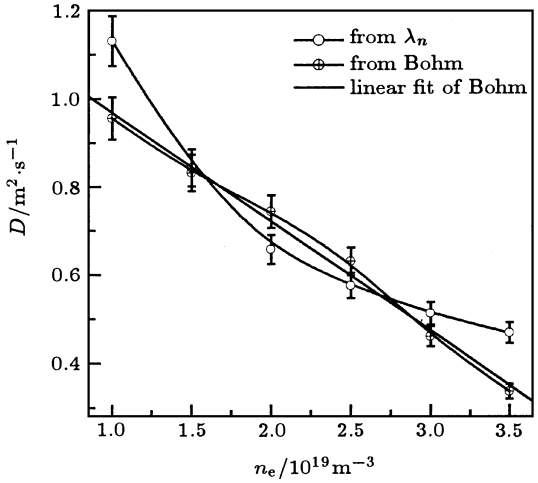


Fig.3. The evolution of $D_\perp$ and $D_\perp^{\rm Bohm}$ with $\bar{n}_e$.

4. Energy distribution of particles

The $H_\alpha(D_\alpha)$ line shape measured by OMA is determined by the convolution of several factors: the instrument function, the geometry of observation, the geometry of the resource, and the effect of atomic and molecular processes. The instrument function can be eliminated by deconvolution, the excited atoms in the n=3 state decay by photon emission on a μs timescale, the exposure time of OMA detector is about 5–8ms, and hence the atomic emission is spatially isotropic. The $H_\alpha(D_\alpha)$ line intensity, within $\Delta\lambda$ from the central wavelength can be written as

$$I(\Delta\lambda) \propto \int n_0 n_e \langle\sigma v\rangle \int_{E(\Delta\lambda)}^{\infty} f(E)/E^{\frac{1}{2}} \mathrm{d}E\mathrm{d}V, \quad (1)$$

where n_0 is the local atomic density, $\langle\sigma v\rangle$ is the excitation rate coefficient for $H_\alpha(D_\alpha)$ emission, $E = mc^2(\Delta\lambda)^2/2\lambda^2$, and the spatial integral is the measuring wavelength region. For T_e higher than 10eV, the number of photons emitted per ionization is approximately constant,[6] and Eq.(1) can be simplified as

$$I(\Delta\lambda) \propto \Gamma_n \int_{E(\Delta\lambda)}^{\infty} f(E)/E^{\frac{1}{2}} \mathrm{d}E. \quad (2)$$

Equation (2) can also be inverted to[7]: $f(E(\Delta\lambda)) \propto \mathrm{d}I(\Delta\lambda)/\mathrm{d}\lambda$. Hence the energy distribution is proportional to the gradient of the $H_\alpha(D_\alpha)$ profile. The result of particle energy profiles in several kinds of experimental conditions is shown Fig.4.

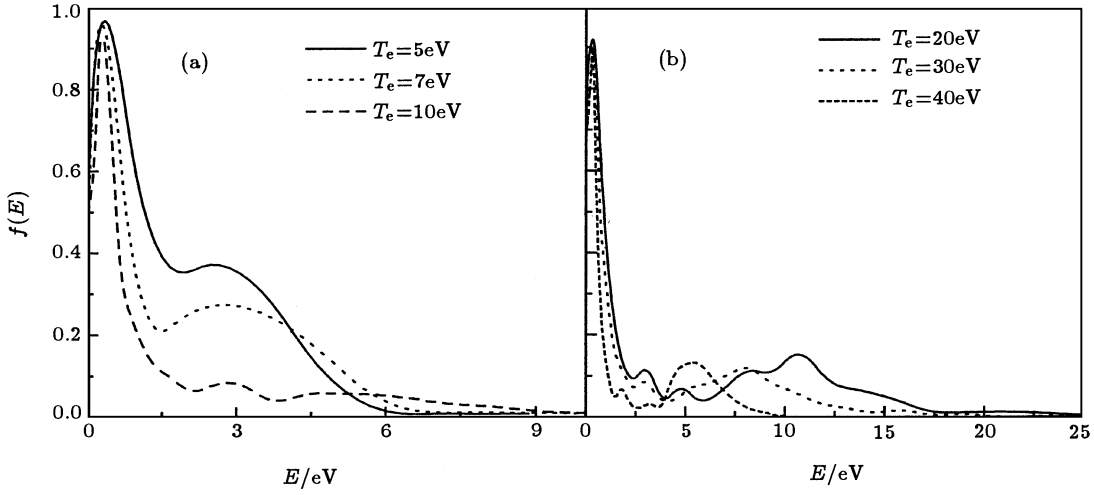


Fig.4. Energy profiles of particles in front of the wall (a) and the limiter (b).

There are two clear peaks in the energy distribution of atoms in front of the wall: the quite strong one is at 0.3eV, which is produced by molecular dissociation excitation. The reaction is $e^- + H_2 \rightarrow e^- + H(1s) + H^*(2s)$.[8] The neutral atoms produced in this reaction have energies ranging from 0 to 1.4eV, peaking at 0.3eV. The average energy loss of the electrons in the collision is about 15.3eV. Another peak is at 3eV, which is produced by molecular dissociation, $e^- + H_2 \rightarrow e^- + H(1s) + H(1s)$.[8] The neutral atoms produced in this reaction have energies ranging from 2 to 6.5eV, peaking at 3eV; the average energy loss in the collision is about 10.5eV, and the peak at 3eV is weaker when the local T_e is above 10eV. The energy profile of the particles in front of the limiter also depends on the experimental condition or local electron temperature. In addition to the peaks at 0.3 and 3eV, another two peaks, at 2.5 and 4.5eV, can be observed when the local T_e is above 20eV; both of them are produced by molecular dissociation excitations: $e^- + H_2 \rightarrow e^- + H(1s) + H^*$ (n=3) and $e^- + H_2 \rightarrow e^- + H^*(2p) + H^*(2s)$.[8] The neutral atoms produced in the two reactions have average energies of 2.5 and 4.8eV; the average energy losses of the electrons in the two collisions are about 21.5 and 34.6eV respectively. A high-energy component lying between 5 and 20eV in the blue wing can always be detected.

5. The result of D_α line shape simulation

The D_α line shape is simulated by calculation based on the Monte Carlo method. During the simulation the background plasma parameters are calculated by the one-dimensional code, in which the fluid equation along the field line in each flux tube is solved under the boundary conditions given by the Langmuir probe, while the ion temperature is assumed equal to the electron temperature and the ion density is also assumed equal to the electron density in front of the limiter or the wall. Several molecular processes, which have been discussed above, are considered in the simulation, and the charge-exchange and reflection of particles have also been considered in the simulation. The Zeeman split is about 0.04nm, while the Doppler broadening of the D_α line is wider than 0.1 nm; therefore the Zeeman effect can be neglected.

So the H_α line in front of the wall can be entirely separated from the D_α line and the ratio of H_α line intensity to D_α line intensity is about 5% in front of the limiter, hence the Zeeman effect and the effect of H_α line are not included in the simulation. The result of the simulation is shown in Fig.5. The simulated D_α line shape agrees with the measured data except for the distribution at the red wing due to the effect of H_α line. The simulation of D_α line shape in front of the wall (Fig.5(a)) shows that the central wavelength shifts 0.015nm to the blue wing. This means that the velocity of particles flowing into the plasma is about $3.0 \times 10^3 \mathrm{ms}^{-1}$, and large emission components are derived from the dissociatively excited and dissociated atoms; they contribute to 82% of the emission and 85% of neutral atoms. The emission profile from the dissociatively excited atoms is symmetrical in this process, whereas the excited atoms decay by photon emission almost instantaneously on a microsecond time scale, without interaction with the plasma and wall. The emission profile from the dissociated atoms is asymmetrical, where the profile is shifted to the blue wing and becomes stronger. This is due to the direction of observation: in this direction the atoms moving to the spectrometer will flow into the core of the plasma, where the density grows higher. The emission from the atoms excited by collision with electrons is stronger. However, the emission from the reflected and charge-exchanged atoms is quite weak; they contribute to 3% of neutral atoms and 13% of emission intensity. The simulated D_α line shape in front of the limiter includes a larger portion of emission components derived from the dissociatively excited and dissociated atoms, and they contribute to 53% emission intensity and about 57% of neutral atoms. Their emission profile is similar to the profile in front of the wall, but the emission from the dissociated atoms is weaker. This is due to the temperature in front of the limiter being higher. The emissions from the reflected and charge-exchanged atoms contribute to 34% and 13% of emission intensity respectively. The rate of particle reflection at the surface of the limiter (R_N) is about 0.47.

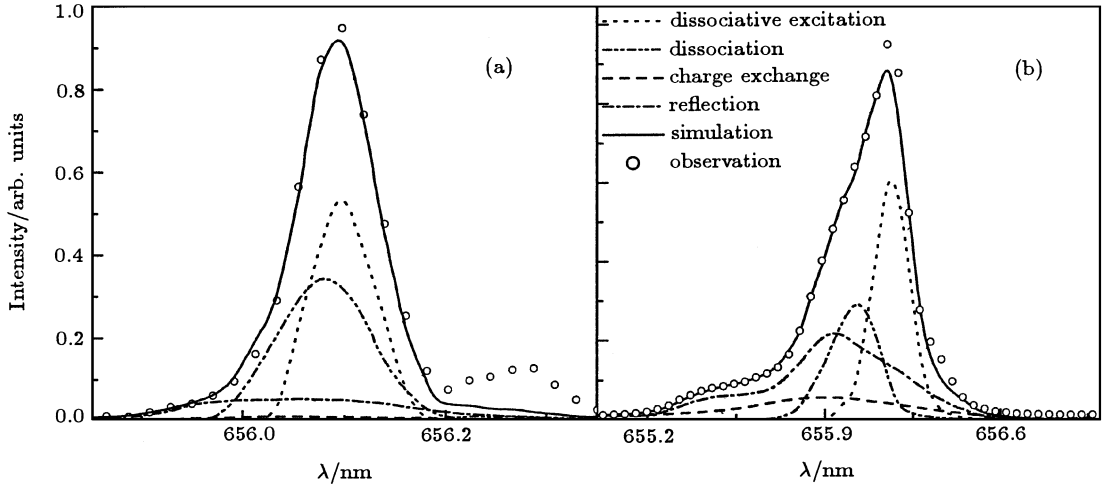


Fig.5. Comparison of the observed D_α line shapes with the simulated ones in front of the wall (a) and the limiter (b).

6. The influence of atomic and molecular processes on the energy balance at the edge

Ions diffuse from the plasma core of a tokamak into the SOL during their flowing towards the limiter. They are accelerated in the plasma sheath layer, gaining an energy of about $3kT_\mathrm{e}$ at the same time, and then neutralized at the surface of the limiter and reflected or absorbed. Atoms reflected into the plasma will have a certain energy of $\frac{1}{2}mv^2 = R_E 3kT_\mathrm{e}$, where R_E is the reflection rate of average energy. The average energy of atoms reflected is about 6, 9 and 12eV at local T_e=20, 30 and 40eV respectively, as shown in Fig.5; therefore R_E is about 0.1. As defined by $Q = \Gamma_n \xi k T_\mathrm{e}$, where Q and ξ are the heat flux at the surface of the limiter and the heat transfer coefficient respectively, Q or ξ can be reduced with increasing fraction of particles reflected.

The molecular density near the limiter and the

wall is significantly high, and the power loss rate per volume can be written as $P = n_e n_0 (\Sigma \langle \sigma v \rangle) \Delta E$, where n_0 is molecular density, $\Sigma \langle \sigma v \rangle \Delta E \approx q \times 10^{-8} (10 + 25\text{eV})$,[9] q is possibly larger than 1, due to the effect of vibrational excitation. At the edge in HT-7 $n_e \approx 2.2 \times 10^{18}\text{m}^{-3}$ and $n_0 \approx 9 \times 10^{16}\text{m}^{-3}$, $q \approx 1$, then the rate of loss of power from molecular dissociation is about $1. \times 10^6 \text{kW}\cdot\text{m}^{-3}$, the ionization depth of the molecular (for $\lambda_{iz} = v_{D_2}/n_e(a) \langle \sigma v \rangle$, $\langle \sigma v \rangle \approx 5 \times 10^{-8}\text{cm}^3\cdot\text{s}^{-1}$) is about 2cm, and the total power loss from the molecular dissociation is about $\pi a^2 2\pi R \lambda_0 P \approx 6 \times 10^4\text{kW}$. Therefore, the molecular dissociation processes play an important role in the energy balance and may control the production of the impurity, especially in front of the wall.

7. Particle behaviour at the edge during IBW heating

Ion Bernstein wave (IBW) heating is based on the fact that the wave excited in the range of ion cyclotron frequency can penetrate into the plasma core without attenuation until it approaches the harmonic cyclotron layers. Ion heating is realized when the wave passes the resonant layers, where the ion cyclotron damping occurs. Ion heating by IBW was observed on JIPP-II-U, [10] PLT. [11] IBW heating was also carried out in HT-7 with an injection power up to 320kW. Particle confinement improvement and direct electron heating was observed in deuterium plasma.[12] A result of typical discharge with IBW is shown in Fig. 6. During IBW heating plasma current does not change, $\bar{n}_e$ rises from $1.0\times10^{19}\text{m}^{-3}$ to $1.2\times10^{19}\text{m}^{-3}$, MHD behaviour is effectively suppressed, and τ_p increase from 9ms to 13ms. The emission of D_α in front of the limiter obviously reduces, but D_α in the front of the wall is almost unchanged. Impurity emission (CIII) and bremsstrahlung emission increase slightly, but effective charge number is almost unchanged because of the increase of n_e.

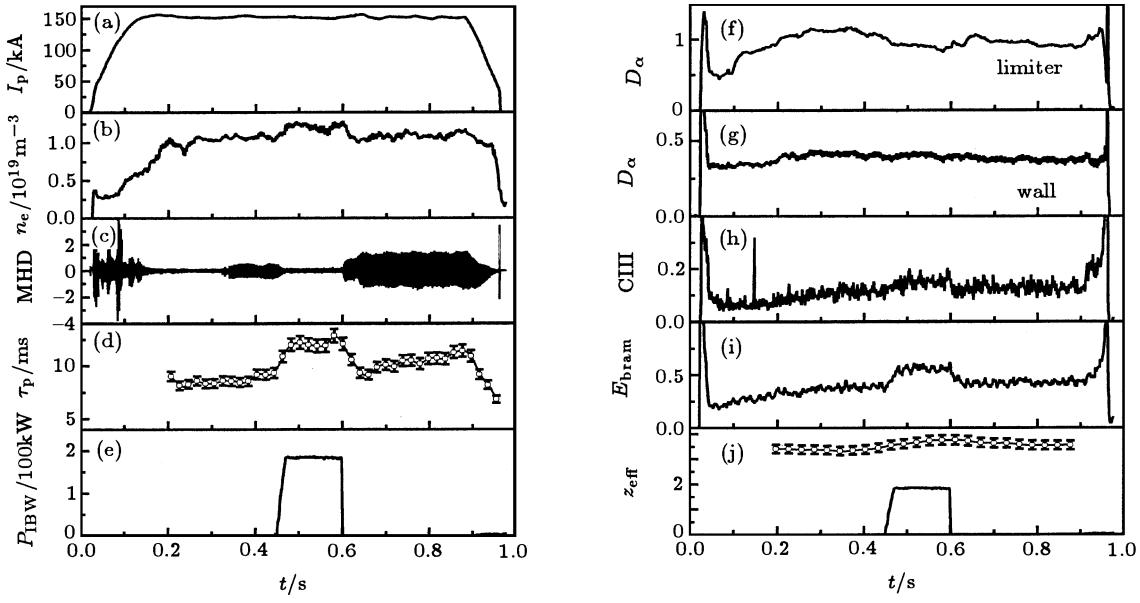


Fig.6. A typical discharge with IBW: (a) plasma poloidal current (I_p). (b) $\bar{n}_e$. (c) MHD. (d)τ_p. (e) IBW injection power (P_{IBW}). (f) The D_α emission from the limiter. (g) The D_α emission from the wall. (h) CIII line emission. (i) Bremsstrahlung emission (E_{brem}). (j) Effective charge number z_{eff}. Note: The units of MHD, D_α, CIII and E_{brem} in Fig.7(c), 7(f), 7(g), 7(h) and 7(i) are arb. units.

The profiles of the electron temperature and density at the edge are shown in Fig.7. The profiles of T_e and n_e become steeper between r=27 and 27.5cm in front of the limiter. λ_e is almost unchanged, but λ_n decreases from 1.85 to 1.1cm, the $D_\perp$ in front of the limiter drops down to $0.2\text{m}^2\cdot\text{s}^{-1}$ and is much lower than the $D_\perp^{\text{Bohm}}$. A transport barrier has more likely formed in front of the limiter, which results in the decrease of the heat flux and the particle flux into the limiter, then the recycling becomes lower and the emission of D_α line reduces clearly in front of the limiter. The profile of T_e and n_e in front of the wall is almost unchanged during ohmic heating and IBW heating, therefore the emission of D_α line and impu-

rity are basically unchanged during IBW heating. The improvement of particle confinement is due to the decrease of $D_\perp$. The IBW heating, which can induce additional sheared poloidal flow in the electron diamagnetic direction and modify the profile of poloidal velocity in the limiter,[13] can suppress the MHD behaviour, the fluctuation levels and the turbulence, and the transport driven by the turbulence will reduce.

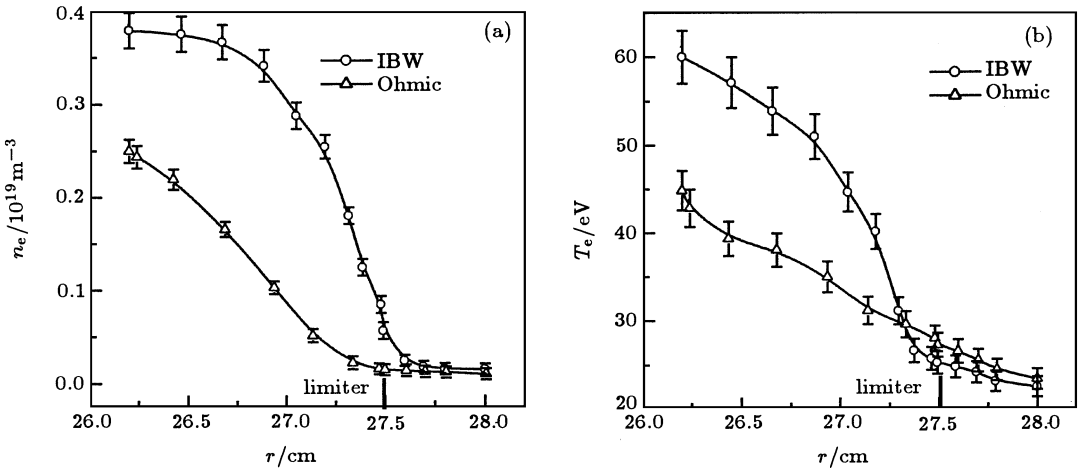


Fig.7. The profile of the electron density (a) and temperature (b) at the edge.

8. Summary

The cross-field diffusion coefficients ($D_\perp$) are quite close to the Bohm diffusion value ($D_\perp^{\rm Bohm}$) at the edge when the $\bar{n}_e$ line is within the range from 1.5×10^{19} to $3.0\times10^{19}m^{-3}$ in HT-7. The particle energy distribution shows that the main molecular processes in the SOL are molecular dissociation excitation, especially when the local T_e is above 10eV, and the reflection rate of the average energy in the limiter is about 0.1. The result of D_α line shape simulation shows that the molecular dissociation contributes to 57% of neutral atoms, 53% of emission intensity in front of the limiter, and to 85% of neutral atoms and 82% of emission intensity in front of the wall. The 47% of the reflection rate of the particles and 10% of the reflection rate of energy will reduce the heat flux in the surface of the limiter, and the power loss from molecular dissociation is about 6×10^4kW. Both of them play an important role for maintaining the balance of energy in the SOL and for controlling impurity resource. The IBW heating can effectively suppress the MHD behaviour, the fluctuation levels and the turbulence. During IBW heating the $D_\perp$ in the limiter clearly decreases from 0.84 to $0.2m^2\cdot s^{-1}$ and the particle confinement time increases from 9 to 12ms.

References

[1] Xie J K, Li J G, Wan B N *et al* 1997 Proc 16th Int. Conf. *Plasma Phys. Control. Nucl. Fusion Rev.* (Montreal) **Vol 1** p685
[2] Wang W H, Yu C X, Wen Z Y *et al* 2001 *Acta Phys. Sin.* **50** 1956 (in Chinese)
[3] Xu W and Wan B H 1998 *Acta Phys. Sin.* **48** 1804 (in Chinese)
[4] Stangeby P and Mccracken G M 1990 *Nucl. Fusion* **30** 1225
[5] Uehara K, Gomay Y, Yamamoto T *et al* 1979 *Plasma Phys.* **21** 89
[6] Wesson John 1997 Tokamaks (Oxford: Clarendon) p431
[7] Ogawa T and Higo M 1979*Chem. Phys. Lett.* **65** 610
[8] Janev R K, Harrison M F A and Drawin H W 1989 *Nucl. Fusion* **29** 109
[9] Janev R K, Post D E, Langer W D and Evans K 1984 *J. Nucl. Mater.* **121** 10
[10] Seki T 1992 *Nucl. Fusion* **32** 2189
[11] Ono M 1988 *Phys. Rev. Lett.* **60** 294
[12] Zhao Y P, Li J G, Luo J R *et al* 2001 *Plasma Phys. Control. Fusion* **43** 343
[13] Wan B N, Song M, Ling B L *et al* 2001 *Nucl. Fusion* **41** 1835